# Measuring the Orbital Angular Momentum of a Single Photon

Jonathan Leach,[1] Miles J. Padgett,[1] Stephen M. Barnett,[2] Sonja Franke-Arnold,[2] and Johannes Courtial[1,*]
[1]Department of Physics and Astronomy, University of Glasgow, Glasgow, Scotland
[2]Department of Physics and Applied Physics, University of Strathclyde, Glasgow, Scotland
(Received 21 January 2002; published 5 June 2002)

We propose an interferometric method for measuring the orbital angular momentum of single photons. We demonstrate its viability by sorting four different orbital angular momentum states, and are thus able to encode two bits of information on a single photon. This new approach has implications for entanglement experiments, quantum cryptography and high density information transfer.

DOI: 10.1103/PhysRevLett.88.257901 PACS numbers: 03.67.–a, 42.50.Ct

It is well known that photons can carry both spin and orbital angular momentum (OAM) [1,2]. The spin is associated with polarization and the OAM with the azimuthal phase of the complex electric field. Each photon of a beam with an azimuthal phase dependence of the form $\exp(il\phi)$, for example, carries an OAM of $l\hbar$. The polarization of a single photon is described by a state in a two-dimensional space. For this reason, photon polarization provides a useful physical realization of a single qubit and has been widely employed in demonstrations of quantum key distribution [3,4]. As recently pointed out [5], the infinite number of orthogonal states of OAM places no limit on the number of bits that can be carried by a single photon. Moreover, the ability to create states with different OAM and superpositions of these allows the realization of quNits, that is quantum states in an $N$-dimensional space, with single photons. The problem addressed in this Letter is the realization of a multichannel device for determining the OAM of a single photon. Such a device will allow us to take advantage of the increase in information capacity associated with orbital rather than spin angular momentum.

Previous work has shown that the OAM of a laser beam containing many photons in the same mode can be measured. For example, interfering an $\exp(il\phi)$ beam with its mirror image produces an interferogram with $2l$ radial spokes [6,7] [Fig. 1(a)]. Although this technique can discriminate between an arbitrarily large number of states, the state of one single photon cannot be measured as many photons are required to form the full interference pattern.

For individual photons, computer-generated holograms [8,9], when used in combination with a pinhole in a setup similar to the one shown in Fig. 1(b), can determine the particular OAM state [10]. Holograms are often used in the generation of $\exp(il\phi)$ beams, where the fork dislocation in the hologram introduces helical phase fronts in the diffracted beam. When operated in reverse, the hologram "flattens" the helical phase fronts. The beam, now with planar phase fronts, can be focused through a pinhole and detected. However, this technique allows photons to be tested only for one particular state. A more complex computer-generated hologram was demonstrated that can detect several different $l$ states but with an efficiency that cannot exceed the reciprocal of the number of different $l$ values [11]. This low efficiency means that this method is not likely to be useful for quantum information applications. In a different approach, the difference in Gouy phase was used within an interferometer to distinguish between modes of two different orders (the mode order is dependent on $l$) [12]. Although working at the single-photon level such a scheme sorts between only two states.

In this Letter we describe an interferometric technique that can distinguish individual photons in arbitrarily many OAM states with a theoretical efficiency of 100%. We demonstrate this principle with a device that simultaneously sorts four different OAM states, corresponding to

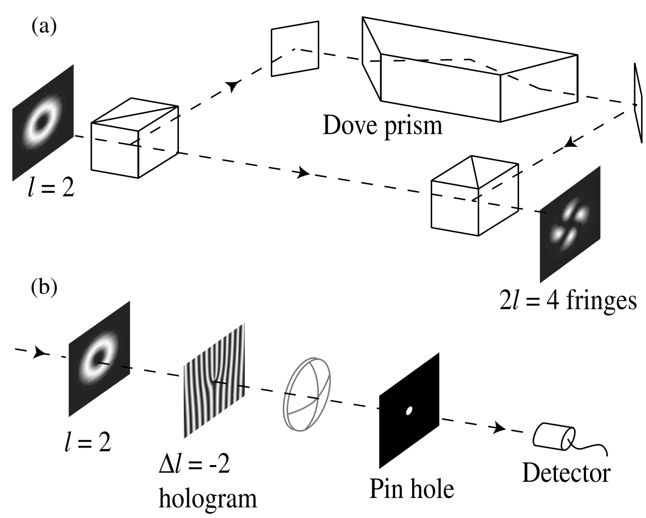


FIG. 1. Previous work on measuring the OAM of light. (a) A Mach-Zehnder interferometer with a Dove prism inserted into one arm interferes the incoming light beam with its own mirror image. In the case of light with $l$ intertwined helical phase fronts, the interference pattern has $2l$ radial fringes. This setup is capable of distinguishing between an arbitrary number of states, but forming the required fringe pattern needs many photons. (b) A hologram can be used to "flatten" the phase fronts of light modes with specific values of $l$, which makes it possible to focus these modes (but no others) through a pinhole, behind which they can be detected. While this latter setup works with individual photons, it can only test for one particular OAM state.

 0031-9007/02/88(25)/257901(4)$20.00  

two bits of information that can be transferred with a single photon.

Our device relies on the $\exp(il\phi)$ form of the transverse modes. On rotation of the beam through an angle $\alpha$, this phase dependence becomes $\exp[il(\phi + \alpha)]$. This corresponds to a phase shift of $\Delta\psi = l\alpha$ [13], which is a manifestation of a geometrical phase [14]. For particular combinations of $l$ and $\alpha$, the rotated beam may be either in or out of phase with respect to the original. For example, when $\alpha = \pi$, a beam with even $l$ is in phase with the original but a beam with odd $l$ rotated by the same angle is out of phase by $\pi$ (Fig. 2). If such a rotation is incorporated into the arms of a two-beam interferometer, then the phase shift between the two arms becomes $l$ dependent. It follows that for different angles of rotation, constructive and destructive interference occurs for different values of $l$.

This concept can be realized in the form of a Mach-Zehnder interferometer with a Dove prism inserted into each arm (Fig. 3). A Dove prism flips the transverse cross section of any transmitted beam [15]. Two Dove prisms, rotated with respect to each other through an angle $\alpha/2$, rotate a passing beam through an angle $\alpha$. In the example shown in Fig. 3, $\alpha/2 = \pi/2$ and hence the relative phase difference between the two arms of the interferometer is $\Delta\psi = l\pi$. By correctly adjusting the path length of the interferometer we can ensure that photons with even $l$ appear in port A1 and photons with odd $l$ appear in port B1. If the input state is a mixture of even and odd $l$ components, then these components are "sorted" into an even channel A1 and an odd channel B1.

Our principle can be extended further to enable us to test for an arbitrarily large number of OAM states. This is achieved by cascading additional Mach-Zehnder interferometers with different rotation angles (Fig. 4). (Note that the scheme outlined in Ref. [12] could be extended in an analogous fashion.) The first interferometer, stage 1, sorts photons with even and odd values of $l$ into ports A1 and B1, respectively. Photons with even $l$ are then passed into the second stage where they are sorted further. The angle between the Dove prisms of the second stage is $\alpha/2 = \pi/4$ corresponding to $\Delta\psi = l\pi/2$. Therefore, modes with $l = 4n$, where $n$ is an integer, go into port A2 and beams with a phase term of $l = 4n + 2$ go into port B2. Unfortunately, there is no rotation angle that allows us to unambiguously sort odd-$l$ photons in the same way. We solve this problem by placing a hologram in front of one interferometer of the second stage so that we can increase the azimuthal phase of the odd-$l$ photons by 1, thereby making their $l$ values even. An additional interferometer with $\alpha = \pi/2$ will now separate the original odd-$l$ photons in the same way as the even-$l$ photons were sorted. Figure 4 outlines the first three sorting stages, which allow discrimination between eight different values of $l$. By adding further stages, this procedure can be extended to allow an arbitrarily large number of OAM states to be distinguished. It should be noted that, in the absence of holograms, a scheme similar to that illustrated in Fig. 4 can be constructed to sort beams where $l$ takes on the values of 0 or $2^n$, where $n$ is an integer.

To demonstrate the viability of our proposed mechanism, three Mach-Zehnder interferometers were built to

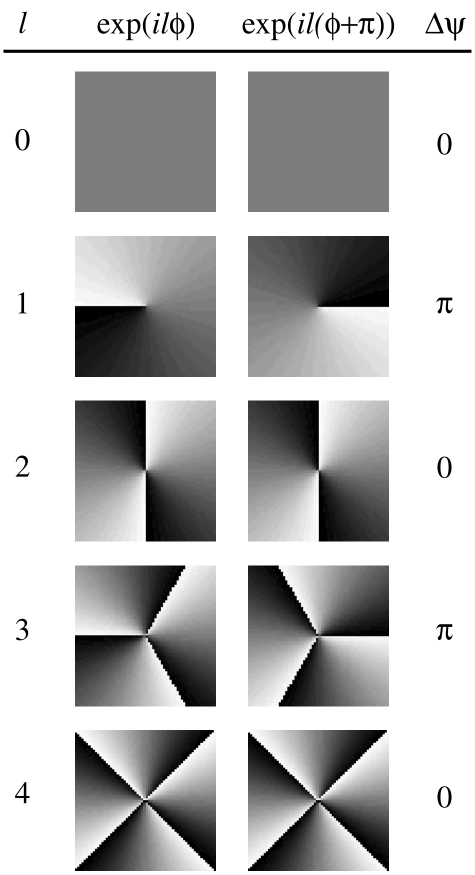


FIG. 2. Gray-scale representations of phase profiles of nonrotated and rotated beams with an $\exp(il\phi)$ phase structure. After a rotation through $\pi$, a beam with even $l$ is unchanged, while one with odd $l$ is out of phase by $\pi$ with the nonrotated beam. Interfering an $l$ beam with a rotated copy of itself therefore results in constructive interference for even $l$ and destructive interference for odd $l$.

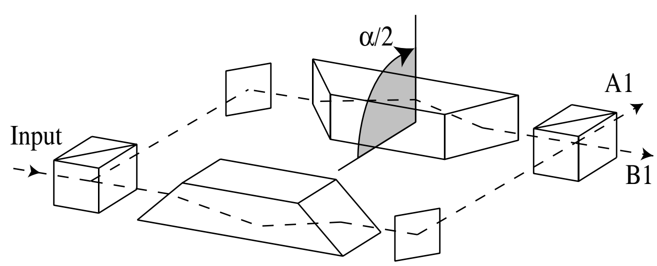


FIG. 3. First stage of our OAM sorter. A Mach-Zehnder interferometer with a Dove prism placed in each arm. The beams in the two arms are rotated with respect to each other through an angle $\alpha$, where $\alpha/2$ is the relative angle between the dove prisms. In the example shown, $\alpha/2 = \pi/2$, this device sorts photons with even values of $l$ into Port A1 and those with odd values of $l$ into Port B1.

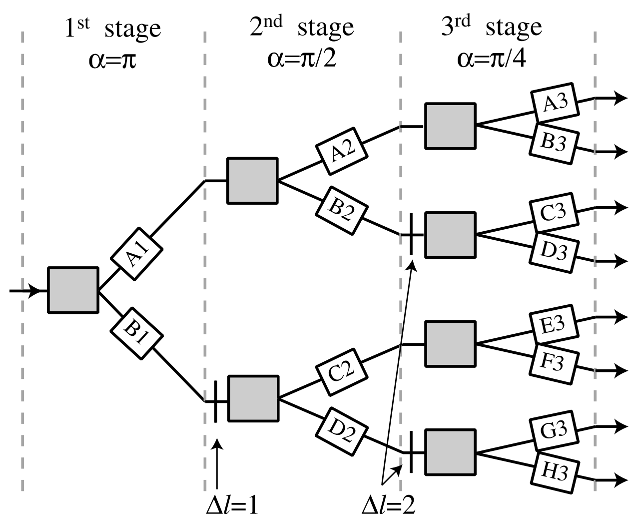


FIG. 4. First three stages of a general sorting scheme. The gray boxes each represent an interferometer of the form shown in Fig. 3 with different angles between the Dove prisms. The first stage introduces a phase shift of $\alpha = \pi$ and so sorts multiples of 2: even $l$s into Port A1 and odd $l$s into Port B1. The odd-$l$ photons then pass though an $\Delta l = 1$ hologram so that they become even-$l$ photons. The second stage introduces a phase shift of $\alpha = \pi/2$, so it sorts even-$l$ photons into even and odd multiples of 2. The $\Delta l = 2$ hologram is required before the photons are sorted further in the third stage.

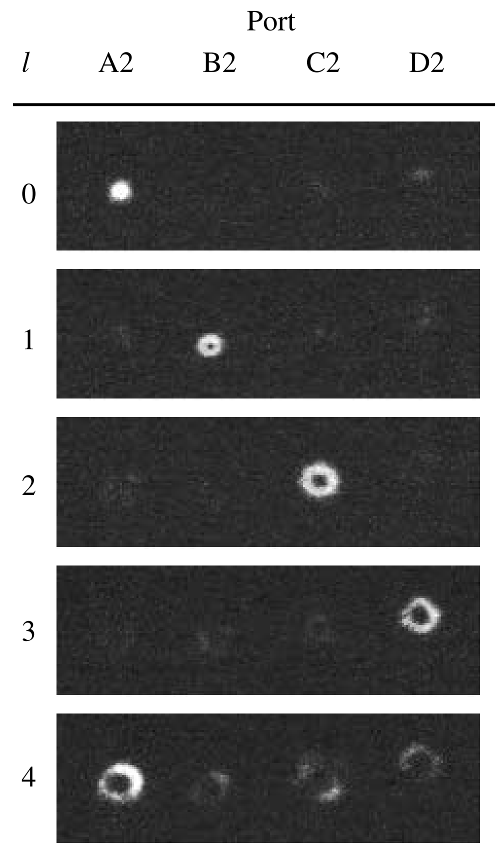


FIG. 5. Experimental results of a 2-stage sorting scheme. The four different output ports correspond to $\exp(il\phi)$ modes with the values $l(\mathrm{mod}4) = 0, 1, 2, 3$, respectively.

form the first two stages of the general OAM sorter outlined in Fig. 4. The light source used in this experiment was a helium-neon laser with a power of <1 mW. An intracavity cross wire introduced rectangular symmetry to the laser cavity and forced the laser to oscillate in high-order Hermite-Gaussian ($HG_{m,n}$) modes. Such modes are characterized by the indices $m$ and $n$ which correspond to zeros of intensity in the electric field in the $x$ and $y$ directions, respectively. The Hermite-Gaussian modes were then converted to Laguerre-Gaussian modes by passing them through a $\pi/2$ mode converter based on cylindrical lenses [16]. The resulting Laguerre-Gaussian modes have an $\exp(il\phi)$ phase structure and corresponding OAM of $l\hbar$ per photon. This conversion of Hermite-Gaussian ($HG_{m,n}$) beams gives Laguerre-Gaussian ($LG_p^l$) beams characterized by $l = |m - n|$ and $p = \min(m, n)$. Adjustments to the intracavity cross wire allowed us to generate $HG_{m,0}$ modes with $m = 0, 1, 2, \ldots,$ which in turn gave rise to $LG_0^l$ beams with $l = 0, 1, 2, \ldots.$ The interferometers had an arm length of approximately 30 cm and were built from standard optical components. The $\Delta l = 1$ hologram was manufactured using standard photographic techniques [17]. Note that such a hologram increases the $l$ value of any $\exp(il\phi)$ mode by 1 [18]. The four ports were directed onto a screen so a camera could take an image of the output.

Figure 5 shows the output from the two-stage sorting process. As can be seen, we succeeded in sorting modes from $l = 0$ to $l = 4$ into different ports. The $l = 4$ mode appears in the same port as the $l = 0$ beam, as one would expect. In this first experiment, the overall efficiency of the OAM sorter was limited by the poor optical efficiency of the particular hologram used to approximately 10%.

To demonstrate that our device works at the single-photon level, a further experiment was carried out at intensities so low that on average less than one photon was present in each interferometer at any one time. This was achieved by inserting neutral-density filters to attenuate the power of the laser beam to <0.3 nW. This experiment used a 1-stage interferometer. The output ports of the interferometer were directed into a camera that averaged over a number of frames. As anticipated, this interferometer still sorts between odd and even $l$s with an efficiency limited only by the quality of the optical components (Fig. 6). Although the device proposed in this Letter can sort individual photons according to their OAM, we did not detect photons individually. We plan to do this in the future with the use of a single photon source and single photon detectors.

Our OAM sorter is the analog of the polarizing beam splitter in that it selects the optical path on the basis of OAM, one path for each of the distinguishable states. In this way, our sorter can be used to generate entanglement between the optical path and OAM in the same way that a polarizing beam splitter can create entanglement between the optical path and polarization [19]. This will make it

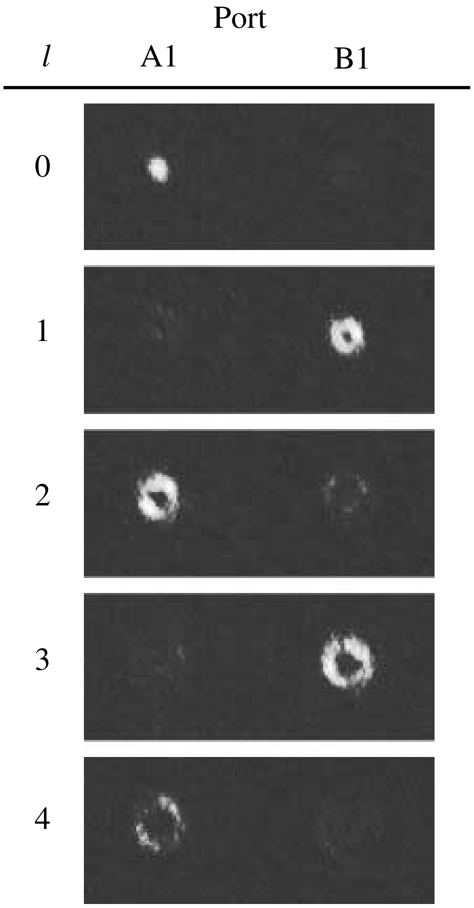


FIG. 6. Experimental results of a 1-stage (even-odd) sorting scheme at the single-photon level. Neutral density filters were used to reduce the number of photons so that the intensity corresponded to one photon in the interferometer at one time.

useful in generating highly entangled states and extending the optical realization of quantum logic elements to OAM quNits [20].

We have demonstrated experimentally that a single photon in an OAM eigenstate can be measured in any one of a number of different orthogonal states corresponding to different values of $l$ (the OAM in units of $\hbar$). Our approach is in principle 100% efficient, limited only by the efficiency of the components.

The ability to measure a single photon to be in any one of an arbitrarily large number of orthogonal states has a number of potential implications for quantum information processing. The efficient measurement of the OAM of a single photon allows us access to a larger state space than that associated with optical polarization. This provides the possibility of a greater density of information transfer along with the generation and analysis of entanglement involving large numbers of states [10]. The implications of this work for entanglement based applications such as superdense coding [21], teleportation [22], and quantum computation [23] remain to be explored.

This work was supported by the Glasgow-Strathclyde University Synergy fund, the Royal Society, the Leverhulme Trust, the Royal Society of Edinburgh, and the Scottish Executive Education and Lifelong Learning Department.

*Electronic address: j.courtial@physics.gla.ac.uk

[1] L. Allen, M.W. Beijersbergen, R.J.C. Spreeuw, and J.P. Woerdman, Phys. Rev. A **45**, 8185 (1992).
[2] L. Allen, M.J. Padgett, and M. Babiker, in *Progress in Optics XXXIX,* edited by E. Wolf (Elsevier Science B. V., New York, 1999), pp. 291–372.
[3] D. Bouwmeester, A. Ekert, and A. Zeilinger, *The Physics of Quantum Information* (Springer, Berlin, Germany, 2000).
[4] S. Pheonix and P. Townsend, Contemp. Phys. **36**, 165 (1995).
[5] G. Molina-Terriza, J.P. Torres, and L. Torner, Phys. Rev. Lett. **88**, 013601 (2002).
[6] M. Harris, C.A. Hill, P.R. Tapster, and J.M. Vaughan, Phys. Rev. A **49**, 3119 (1994).
[7] M.J. Padgett, J. Arlt, N.B. Simpson, and L. Allen, Am. J. Phys. **64**, 77 (1996).
[8] V.Y. Bazhenov, M.V. Vasnetsov, and M.S. Soskin, JETP Lett. **52**, 429 (1990).
[9] N.R. Heckenberg, R. McDuff, C.P. Smith, and A.G. White, Opt. Lett. **17**, 221 (1992).
[10] G. Weihs and A. Zeilinger, Nature (London) **412**, 313 (2001).
[11] V.V. Kotlyar, V.A. Soifer, and S.N. Khonina, J. Mod. Opt. **44**, 1409 (1997).
[12] M.V. Vasnetsov, V.V. Slyusar, and M.S. Soskin, Quantum Electron. **31**, 464 (2001).
[13] J. Courtial, D.A. Robertson, K. Dholakia, L. Allen, and M.J. Padgett, Phys. Rev. Lett. **81**, 4828 (1998).
[14] M.J. Padgett and J. Courtial, Opt. Lett. **24**, 430 (1999).
[15] M. Born and E. Wolf, *Principles of Optics* (Pergamon Press, Oxford, 1980), 6th ed.
[16] M.W. Beijersbergen, L. Allen, H.E.L.O. van der Veen, and J.P. Woerdman, Opt. Commun. **96**, 123 (1993).
[17] J. Arlt, K. Dholakia, L. Allen, and M.J. Padgett, J. Mod. Opt. **45**, 1231 (1998).
[18] If the incident mode is an LG mode, which is of the form $\exp(il\phi)$, the transmitted beam is no longer a pure LG mode, but is still of the form $\exp(il'\phi)$ (with $l' = l + 1$). There is no fundamental reason limiting the holographic conversion of $\exp(il\phi)$ modes, but in practice they currently convert at best about 85% of the incident power.
[19] T.J. Herzog, P.G. Kwiat, H. Weinfurter, and A. Zeilinger, Phys. Rev. Lett. **75**, 3034 (1995).
[20] N.J. Cerf, C. Adami, and P.G. Kwiat, Phys. Rev. A **57**, R1477 (1998).
[21] C.H. Bennett and S.J. Wiesner, Phys. Rev. Lett. **69**, 2881 (1992).
[22] C.H. Bennett, G. Brassard, R. Jozsa, A. Peres, and W.K. Wootters, Phys. Rev. Lett. **70**, 1895 (1993).
[23] M.A. Nielsen and I.L. Chuang, *Quantum Computation and Quantum Information* (Cambridge University Press, Cambridge, United Kingdom, 2000).